

PACS numbers: 42.55.Rz; 42.55.Lt; 42.60.By; 42.60.Jf; 42.65.Jx; 42.65.Re
DOI: 10.1070/QE2014v044n05ABEH015442

Ti:sapphire/KrF hybrid laser system generating trains of subterawatt subpicosecond UV pulses

V.D. Zvorykin, A.A. Ionin, A.O. Levchenko, G.A. Mesyats, L.V. Seleznev, D.V. Sinitsyn, N.N. Ustinovskii, A.V. Shutov

Abstract. **The GARPUN-MTW Ti:sapphire/KrF hybrid laser system is used to investigate different multipass schemes for amplifying trains of ultrashort pulses (USPs) of subpicosecond duration. It is shown that, for an USP repetition period of 3–5 ns, which exceeds the gain-medium recovery time (~2 ns), trains are amplified in the same way as single USPs. Due to this, a train can efficiently extract pump energy from the amplifier and sum energies of individual USPs. The energy of a four-USP train, extracted during four passes through the preamplifier and two passes through the final KrF amplifier (4+2 scheme), is saturated at a level of 1.6 J and corresponds to maximum USP peak powers of about 0.6 TW. The energy of amplified spontaneous emission (ASE), on the contrary, rapidly increases at a large total gain length $L_{\rm eff} \approx 6$ m and is approximately equal to the USP energy. In the (4+1) and (2+2) schemes the USP energy decreases only slightly, to $E_{\rm out} = 1.3$ and 1.2 J, and the ASE fraction is reduced to about 10% and 3%, respectively. USP self-focusing leads to multiple laser beam filamentation and a 200-fold local increase in the radiation intensity in filaments, to $\sim 2\times10^{11}$ W cm^{-2}, a level at which the nonlinear loss in the output CaF_2 windows of the KrF amplifier, caused by three-photon absorption, nonlinear scattering, and broadening of the radiation spectrum to a value exceeding the gain band of the KrF laser transition, becomes the main factor determining the saturation of the USP output energy.**

Keywords: *amplification of subpicosecond subterawatt pulses in KrF amplifiers, multipass amplification schemes, nonlinear loss in amplifier windows.*

1. Introduction

Twenty-year studies with KrF lasers (see, for example, [1, 2] and references therein) led to development of different facilities for generating ultrashort pulses (USPs) in the UV range. Among them, the most promising appear to be hybrid systems, where USPs are generated by a Ti:sapphire master oscillator and, after frequency tripling, amplified at the wavelength $\lambda = 248$ nm in KrF amplifiers [3–5]. As compared with solid-state amplifiers of chirped USPs, which operate in the IR region (see, for example, [6, 7]), KrF lasers have a relatively low saturation energy $Q_{\rm s} = h\nu/\sigma \cong 2$ mJ cm^{-2} and a limited gain bandwidth $\Delta\lambda_{1/2} \approx 2.5$ nm ($h\nu = 5$ eV and $\sigma = 2.5\times10^{-16}$ cm^2 are, respectively, the energy and cross section of the laser transition [8]); however, when pumped by relativistic electron beams, they may have gain media of very large sizes, which makes it possible to obtain subpicosecond UV USPs with a peak power of a few terawatts [9–11]. Being inferior to solid-state systems with respect to limiting durations and peak powers, hybrid Ti:sapphire/KrF laser systems have, nevertheless, a significant advantage in the case of direct amplification of a train of UV USPs or amplitude-modulated pulses, which is a combination of USPs regeneratively amplified in an unstable cavity and a 100-ns free lasing pulse [12]. This unique possibility is provided by fast relaxation processes occurring in the gain medium of the KrF laser, which recover the population inversion on the laser transition over a time $\tau \sim 2$ ns after the passage of the previous USP [8, 12, 13].

As was shown in [14, 15], amplitude-modulated pulses efficiently ionise atmospheric air due to the high peak power of USPs and high energy of UV photons. At the same time, the long emission pulse maintains the electron density in the air plasma, preventing electrons from attaching to oxygen molecules. This leads to the formation of relatively long-lived plasma channels, which are of interest for controlling extended electric discharges [15, 16] and directed transfer of microwave radiation through hollow plasma waveguides [17].

The possibilities of scaling KrF amplifiers to energies of several tens of kilojoules at high (to 7%) total efficiency and their long-term non-stop operation with a pulse repetition frequency $f \sim 10$ Hz in combination with the short wavelength and wide spectrum of amplified radiation (which provides a higher ablation pressure and stable compression of thermonuclear targets) are undoubted advantages of KrF drivers in the developed energy facilities based on inertial confinement fusion (ICF) (see, for example, [18]). For the most efficient, so-called separate compression and fast ignition of ICF targets by particles accelerated in a plasma or by a high-power shock wave, one must apply temporal profiling of nanosecond pulses with a sharp increase in the radiation power by two orders of magnitude during the last several tens of picoseconds. In the case of KrF drivers these pulses can be obtained as a result of summation of separately amplified short and long pulses directly on a target [2, 11] or during their simultaneous amplification in amplifiers [1, 13, 19–21].

The amplification of single USPs with a duration $\tau \ll \tau_{\rm c}$ in a single-pass KrF amplifier in the incoherent regime is described by the modified Franz–Nodvik equation [22]

$$\frac{{\rm d}\varepsilon}{{\rm d}x} = g(x)[1 - \exp(-\varepsilon)] - \alpha_{\rm ns}\varepsilon, \qquad (1)$$

V.D. Zvorykin, A.A. Ionin, A.O. Levchenko, G.A. Mesyats, L.V. Seleznev, D.V. Sinitsyn, N.N. Ustinovskii, A.V. Shutov P.N. Lebedev Physics Institute, Russian Academy of Sciences, Leninskii prosp. 53, 119991 Moscow, Russia; e-mail: zvorykin@sci.lebedev.ru

Received 3 March 2014
Kvantovaya Elektronika **44** (5) 431–439 (2014)
Translated by Yu.P. Sin'kov

where $\varepsilon = Q/Q_s$; $I(x,t)$ and $Q(x) = \int_0^\tau I(x,t')\,dt'$ are, respectively, the intensity and energy density of USPs propagating through the amplifier; and $g(x)$ is the gain distribution, which is formed by amplified spontaneous emission (ASE) [1]. The highest gain efficiency at $g(x) \approx g_0$ is obtained for the energy density $Q_{opt} = Q_s \ln(g_0/\alpha_{ns}) = 4.6–6.0$ mJ cm^{-2} (here, $g_0/\alpha_{ns} = 10–20$ is the ratio of the small-signal gain to the nonsaturable-absorption coefficient of laser radiation in a gain medium) [5, 12]. Under these conditions, a single USP extracts the excitation energy accumulated over the time $\tau_c \sim 2$ ns, which is short in comparison with the characteristic duration of electron beam pumping, $\tau_p \sim 100$ ns, and the electro-optical (internal) amplifier efficiency does not exceed few tenths of percent. For a train of USPs following with an interval $\Delta t \sim \tau_c$, the highest efficiency is implemented for $Q_{opt} = 3.1–4.3$ mJ cm^{-2} and, provided that the train duration is equal to the amplifier pump duration, the electro-optical efficiency increases to 10%–12%. When USPs are amplified in large KrF amplifiers, one must take into account gain saturation by the ASE [1, 5] and, in the case of multipass scheme, the interference of oppositely propagating USPs.

This work, which is a continuation of [5, 12, 21], is devoted to the analysis and optimisation of multipass amplification of a UV USP train on the GARPUN-MTW Ti:sapphire/KrF hybrid laser system and to experimental determination of the energy limit of amplified radiation and the factors influencing it.

2. Amplification of USP trains in KrF amplifiers of the GARPUN-MTW laser facility

2.1. Main elements

The GARPUN-MTW Ti:sapphire/KrF hybrid laser facility, which was described in detail in [1], consists of two cascades of KrF amplifiers with electron beam pumping – the final large-aperture GARPUN amplifier with a gain-medium volume of 12×18×100 cm and Berdysh preamplifier (8×8×110 cm); an auxiliary electric-discharge TMSC 150 KrF laser (Lambda Physik EMG), which is used to lock amplifier pumping; and a Ti:sapphire Start-248M front-end (Avesta Project Ltd.). The front-end generates UV USPs, the energy of which (after the frequency conversion to the KrF gain band) amounts to 0.5 mJ at a pulse width of ~100 fs. The front-end generally operates with a frequency $f = 10$ Hz. This regime was used to align the tract of KrF amplifiers and the detecting units. In the USP amplification regime, a single USP, synchronised using KrF-amplifier pumping with an error of ±5 ns, was cut from a continuous USP sequence by an electromechanical shutter. The entire system was synchronised by the front-end clock generator. This generator triggered (via digital delay generators) the pulsed high-voltage supply of KrF amplifiers and the auxiliary KrF laser, which, in turn, ignited dischargers of the pulse forming lines of vacuum diodes used to generate pump electron beams.

To obtain a train, a single USP was introduced into a mirror ring multiplexer, formed by three flat highly reflecting mirrors and a beam splitter (a thin CaF_2 plate with a dielectric coating) [12]. For a beam splitter with 30% reflection, the total train energy E reached 0.1 mJ, and the energies of individual USPs in train obeyed the ratio $E_1:E_2:E_3:E_4\ldots = 3:5:1.5:0.5\ldots$. The choice of the USP repetition period was determined by the gain recovery time in the gain medium of KrF laser, $\Delta t \geqslant \tau_c$, and varied from 3 to 5 ns by changing the distance between the multiplexer mirrors. With the delay line shuttered, there was only the first USP of the train at the multiplexer output, which contained $E_1/E \approx E_1/(E_1 + E_2 + E_3 + E_4) =$ 30% of the total train energy. The output beam ~8 mm in diameter could be passed through a pair of step diffraction attenuators, which discretely reduced the USP energy by a factor of up to 1000, after which the beam was increased in diameter by a factor of 3 (using a mirror telescope) and directed to the amplifier chain.

2.2. Successive double-pass amplification of a USP train in Berdysh and GARPUN amplifiers (2+2 scheme)

We experimentally investigated different schemes of USP train amplification. The basic configuration (Fig. 1) implies two passes in the Berdysh preamplifier and two subsequent passes in the final GARPUN amplifier (2+2 scheme) [5, 21]. To reduce the ASE interference, which arose in each amplifier, a vacuum spatial filter (having a length of 6 m and a symmetrically located diaphragm) was inserted between the amplifying cascades. The amplifier windows and the spatial filter, as well as the lenses of the additional spatial filter, which was used in the four-pass preamplifier scheme (see Subsection 2.3), were made of high-purity calcium fluoride (FKU grade). Windows without antireflection coatings were tilted at a small angle to the optical axis to exclude parasitic generation. All other elements of the optical track were highly reflecting mirrors with dielectric coatings deposited on KU-1 quartz substrates. They were used to direct the laser beam along the amplification track; the beam cross section was matched with the apertures of amplifiers and spatial filters. The amplified USPs and ASE were monitored by coaxial vacuum FEK 29 KPU photodiodes with a time resolution of ~1 ns, the signals of which were recorded with a four-channel Tektronix TDS-3054 digital oscilloscope with a sampling rate of 5 GHz. Photodiode PD1 was placed behind the highly reflecting preamplifier mirror, and photodiodes PD2 and PD3 were installed behind the turning mirrors at the output of the spatial filter and final amplifier. Note that the attenuation of the USPs transmitted through the mirrors, caused by two-photon nonlinear absorption in quartz, multiply exceeds the ASE attenuation. In addition, because of the limited time resolution, photodiodes integrated USPs over duration (according to the measurements by an electron-optical camera [5, 21], it did not exceed $\tau \sim 1$ ps) and underestimated the true

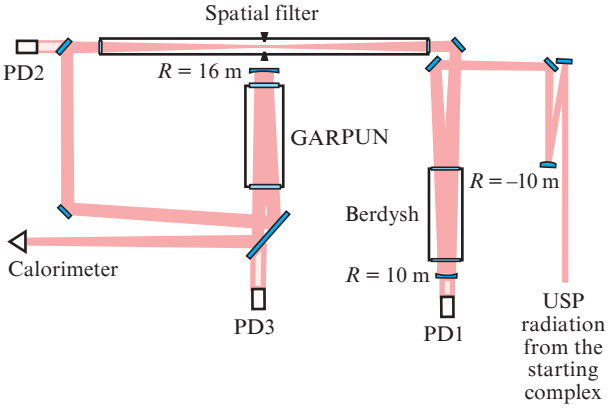

Figure 1. Scheme of double-pass USP amplification in the Berdysh preamplifier and GARPUN amplifier (2+2).

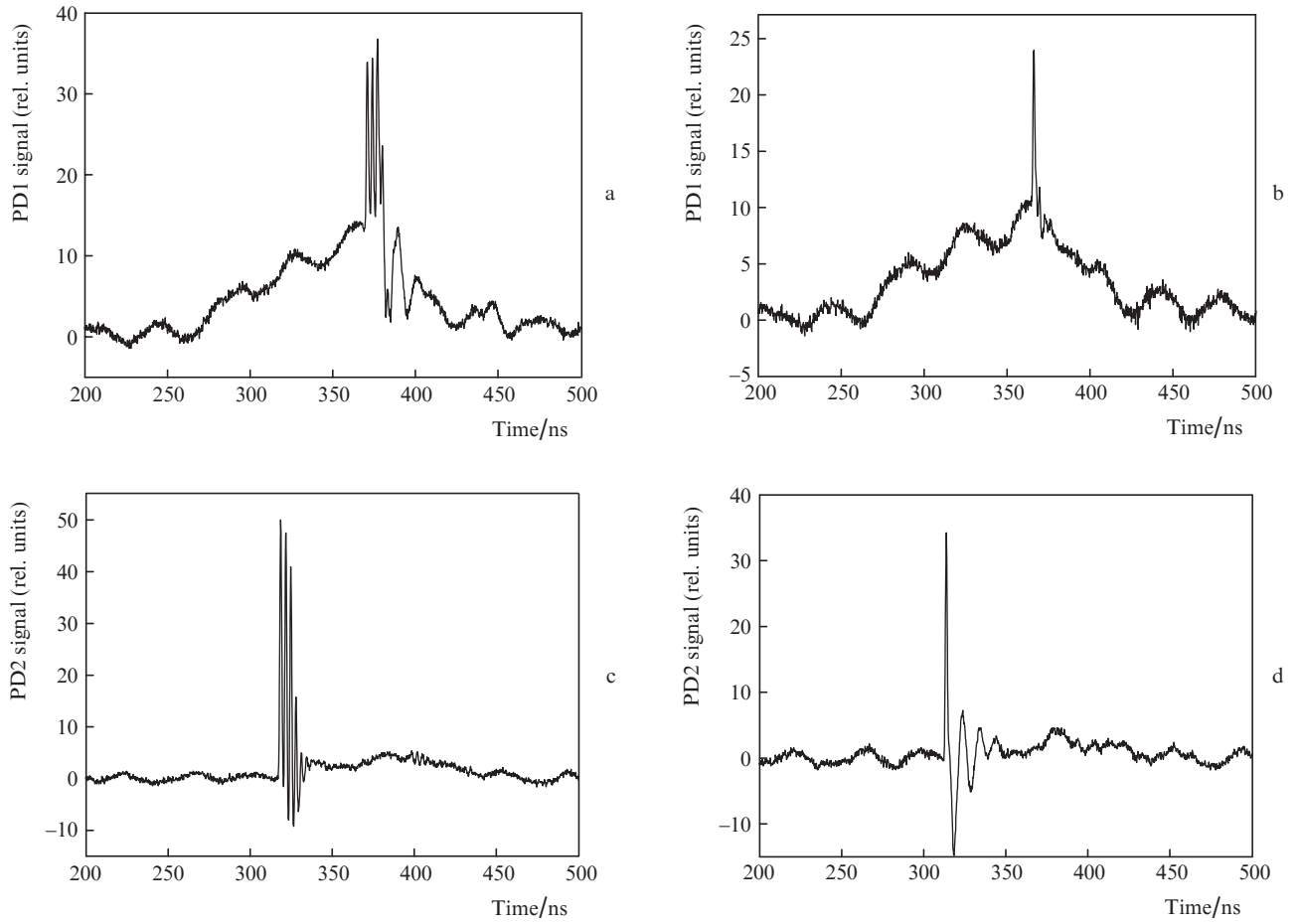

Figure 2. Oscillograms of signals from photodiodes (a, b) PD1 and (c, d) PD2 for amplification of (a, c) USP train and (b, d) single USP in the (2 + 2) scheme. Time is counted from the oscilloscope sweep reference point.

USP amplitude by a factor of at least 1000. The oscillograms (Fig. 2) exhibited significant overoscillations (which were especially significant in the case of single USPs), caused by the nonlinear response of photodiodes to high-power short light pulses. For this reason, photodiodes were only used to control the locking of amplifiers and USPs. Quantitative measurements of the USP and ASE energy were performed using a calorimeter; the ASE contribution was determined without USP injection into the amplification channel. The calorimeter was placed in a weakly focused beam at a distance of 10 m from the final-amplifier output, and only a small fraction of ASE, propagating in a larger solid angle, rather than amplified USPs, arrived at a receiving area 2 cm in diameter [1].

To choose the optimal time for introducing a USP train into amplifiers (in order to attain the highest USP energy at the output), we performed two series of preliminary measurements; in each series one of the amplifiers operated in the standard regime, whereas the other operated in the no-load regime (i.e., without pumping). At the same time, we varied the delay between the pump pulse (specifically, the ASE pulse) and the USP train, which was monitored by photodiodes; the radiation energy was measured by a calorimeter. Figure 2 shows typical signals from photodiodes PD1 and PD2 for the cases of amplification of a USP train and a single USP (with a shuttered delay line in the multiplexer) in the Berdysh preamplifier. The signal from photodiode PD1, which was located behind the highly reflecting mirror of the preamplifier, consists of a USP, amplified in the first pass against the background of a long ASE pulse. One can see how the USP train saturates amplification in the gain medium, which is accompanied by a decrease in the ASE power. Photodiode PD2, which detects the radiation transmitted through a spatial filter, can record only the USP, because a large fraction of ASE, propagating at large angles to the optical axis, is cut off by the filter diaphragm. When pumping the main GARPUN amplifier, photodiode PD3, which was mounted not far from the output amplifier window (behind the highly reflecting turning mirror (see Fig. 1), recorded a superposition of an amplified USP and ASE (see Fig. 7); at large (10 m) distances from the amplifier (i.e., in the region where the calorimeter was located), only USP was recorded.

The dependence of the radiation output energy (measured by calorimeter) on the input energy of the USP train amplified in the double-pass amplification scheme (2 + 2) is shown in Fig. 3. The USP repetition period in these experiments was ~5 ns. The total energy consists of the output energy of the amplified USP train and the ASE energy. The latter was measured without injecting a USP train into amplifiers and did not exceed few percent of the total energy. The ASE energy is shown by a thin horizontal line. Hereinafter, unless otherwise indicated, we present the results of measurements carried out with freshly prepared working gas mixtures in amplifiers.

A dependence qualitatively similar to that presented in Fig. 3 was obtained in the (2+2) amplification scheme and

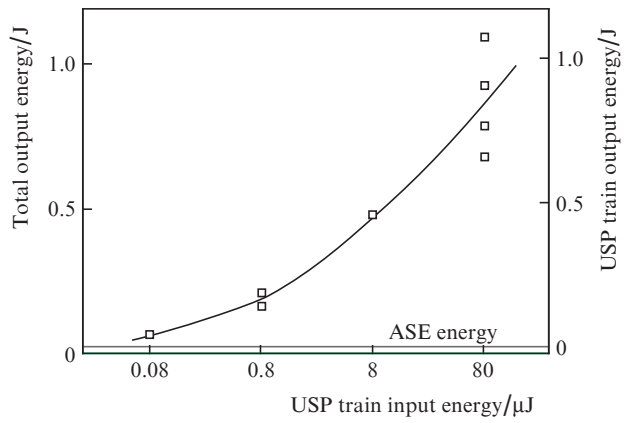

Figure 3. Dependences of the total output energy and the output energy of amplified USP train on the USP train input energy for the double-pass scheme of USP amplification in the Berdysh preamplifier and GARPUN amplifier (2+2).

for single USPs, with the only difference: their energy was on average lower by a factor of 2.5 than the total train energy. The oscillograms in Fig. 2 indicate [see also oscillograms in Fig. 7 for the (4+2) amplification scheme] that the train contains four USPs, which make the main contribution to the measured energy. Having compared the found ratio of the train and single USP energies with the corresponding ratio at the multiplexer output (~3), one can conclude that individual USPs in a train, which followed with an interval $\Delta\tau \sim 5$ ns, were amplified approximately in the same way as single USPs. The trend to equalisation of the amplitudes of amplified USPs in the oscillograms is indicative of gain saturation. The redistribution of the USP energy can also be explained by the change in the gain-medium during the time of train propagation through the amplifiers and the error of multiplexer tuning, because poor alignment of the multiplexer scheme leads to increasing deviation of subsequent train pulses from the optical axis of the amplification channel and their possible cutoff by the spatial-filter diaphragm. In addition, the first USP in the train, when amplified in the double-pass scheme, gains some advantage over the others, the amplification of which in the first pass is affected by the saturation of the medium induced by the previous train pulses, propagating in the opposite direction and, therefore, having a higher power.

For a train with an energy E_{in} ~0.08 mJ at the amplifier input, the maximum output energy E_{out} was 1.2 J and the maximum single-USP energy reached 0.4 J (at an input energy of ~0.025 mJ). Previously, amplification of single USPs with the input energy $E_{in} = 0.32$ mJ in the same double-pass scheme yielded an output energy $E_{out} = 0.6$ J at an energy density $Q_{out} = 6.7$ mJ cm^{-2}, which is close to the optimal value obtained from Eqn (1) [5, 21]. Thus, the significant (by more than an order of magnitude) decrease in the single-USP energy at the amplifiers input, caused by the multiplexer, decreased the output USP energy by a factor of only 1.5, i.e., the final amplifier operated in the close-to-saturation regime. When a USP train was amplified, the output energy, on the contrary, was doubled due to the summation of individual pulse energies. One would expect the implementation of two additional USP passes through the preamplifier to compensate for the energy loss in the multiplexer and increase the output-train energy.

2.3. Four-pass amplification of a USP train in the Berdysh preamplifier with subsequent single-pass (4+1 scheme) or double-pass (4+2 scheme) amplification in the GARPUN amplifier

We investigated different optical schemes with two additional passes through the Berdysh preamplifier in order to increase the USP train output energy. Two amplification versions [with one (4+1 scheme) or two (4+2 scheme) subsequent passes through the main GARPUN amplifier] are shown in Fig. 4. The USP input beam with a diameter of ~30 mm was passed twice through the amplifying medium of the preamplifier and then passed through a vacuum spatial filter, which was additionally installed in the scheme to exclude excitation of generation. The focal lengths of lenses L1 and L2 and the lengths of the spatial filter shoulders were chosen so as to make the latter form a divergent beam, completely filling the preamplifier aperture in the subsequent two passes. The energy of the USP train amplified in the preamplifier was measured by a calorimeter placed behind the main spatial filter; the measured value corresponded to the energy arriving at the main-amplifier input.

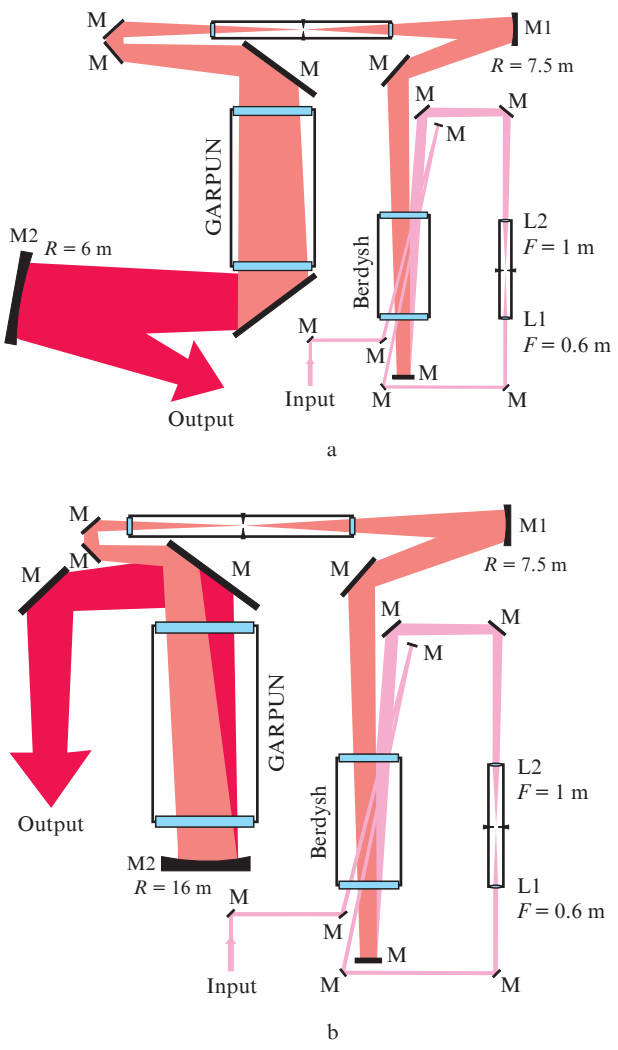

Figure 4. USP amplification with four passes through the Berdysh preamplifier and (a) one (4+1) or (b) two (4+2) passes through the GARPUN amplifier.

Figure 5 shows a dependence of the total output energy of a USP train after four passes through the Berdysh preamplifier on the input train energy. The maximum output energy is $E_{out} = 0.13$ J at $E_{in} = 0.08$ mJ; this value corresponds to the total gain $G = E_{out}/E_{in} \approx 1600$ after four passes. The ASE energy measured in this scheme turned out to be rather low: $E_{ASE} \sim 3$ mJ. For comparison, we obtained a single USP energy $E_{out} = 23$ mJ at $G \approx 70$ after the preamplifier in our previous experiments with the double-pass scheme [5, 21].

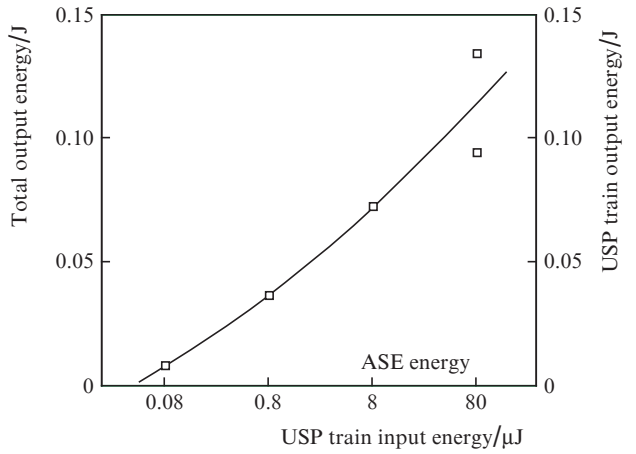

Figure 5. Dependences of the total output energy after the Berdysh preamplifier and the output energy of amplified USP train on the USP train input energy for the scheme with four passes through the Berdysh preamplifier.

Figure 6 shows dependences of the total output energy and the output energy of USP train (with the subtracted ASE) on the input energy of the USP train for the (4 + 1) and (4 + 2) amplification schemes. Typical oscillograms of signals from photodiodes PD1 and PD3 for the (4 + 2) scheme are shown in Fig. 7a. These oscillograms, being superpositions of amplified USPs and ASE, as was noted in Subsection 2.2, were used to monitor USP locking and pumping of amplifiers. In the double-pass (4 + 2) scheme, the ASE contribution to the total radiation energy is about 50% (Fig. 6a), which is larger by a factor of about 5 than that in the single-pass (4 + 1) scheme (Fig. 6b). The increase in ASE in the (4 + 2) scheme, which is caused by exponential ASE amplification and twofold increase in the effective length of the final amplifier ($I_{ASE} \propto \exp[(g_0 - \alpha_{ns}) L_{eff}]$), is in agreement with the measurement and calculation results [1]. At the same time, the energy of the amplified USP train changes only slightly, because USPs are amplified in the saturated regime. A similar behaviour is observed for the amplification in the (4 + 2) scheme, where a large number of pump pulses leads to the working mixture degradation with the corresponding decrease in gain g_0 and increase in the intrinsic absorption α_{ns} of the gain medium (Fig. 6c). The increase in the ASE intensity in the double-pass scheme leads to saturation of gain and its decrease on average by a factor of 2.5 with respect to the small-signal gain $g_0 \sim 0.08$ cm^{-1} [1]. For comparison, the gain in the single-pass scheme decreases on average to $\sim$0.05 cm^{-1} because of the saturation by the ASE. In addition, a small part of spontaneous radiation from the preamplifier, amplified in the four-pass scheme, arrives (despite the cutoff by spatial filters) in the form of a seed at the input of the final amplifier and is amplified in it, along with the intrinsic ASE. For example, the oscillograms in Fig. 7b, obtained in the absence of USPs at the input of amplifiers, exhibit an increase in the ASE power in the final amplifier at the instant when the ASE from the preamplifier enters it.

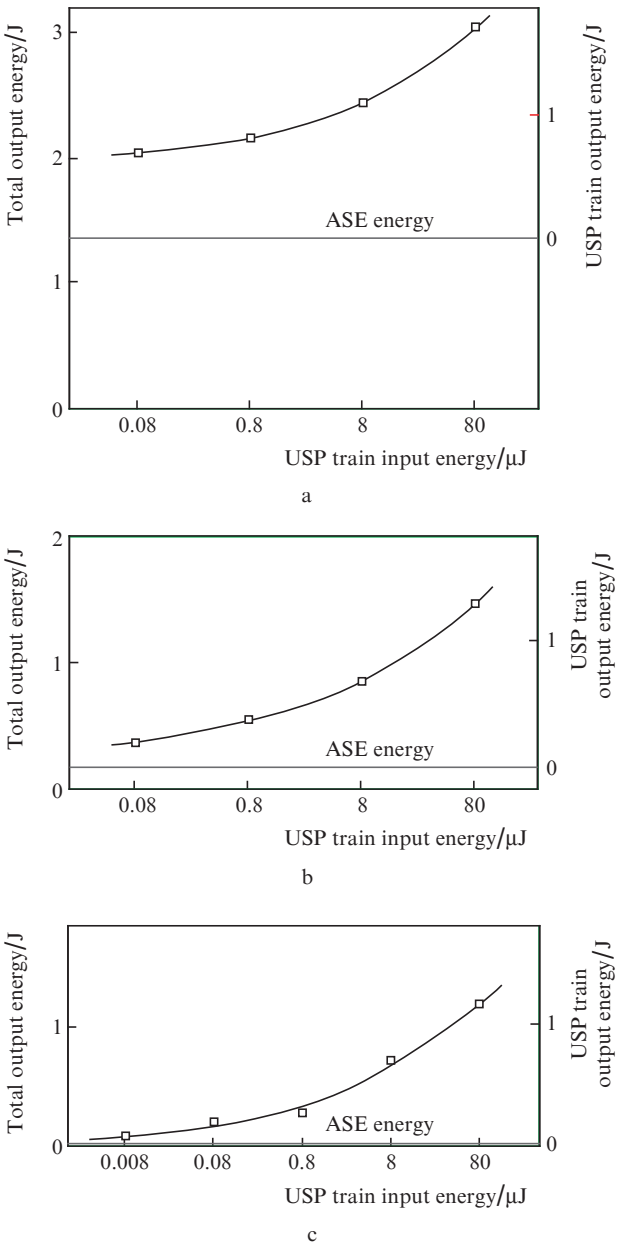

Figure 6. Dependences of the total output energy after the Berdysh and GARPUN amplifiers and the output energy of amplified USP train on the USP train input energy in schemes with (a) four passes through Berdysh and two passes through GARPUN; (b) four passes through Berdysh and one pass through GARPUN (4 + 1); and (c) four passes through Berdysh and two passes through GARPUN (4 + 2), filled with a long-term used gas mixture.

As a whole, all dependences in Fig. 6 are qualitatively similar: an increase in the input USP energy by three orders of magnitude increases the output energy only a few times. The largest gain saturation was observed for the (4 + 2) scheme, which provided a maximum energy of the amplified USP train: 1.6 J. In the (4 + 1) amplification scheme, the maximum train energy was 1.3 J, a value little differing from the energy 1.2 J, measured in the double-pass scheme (2 + 2). Thus, under the conditions of USP gain saturation, the

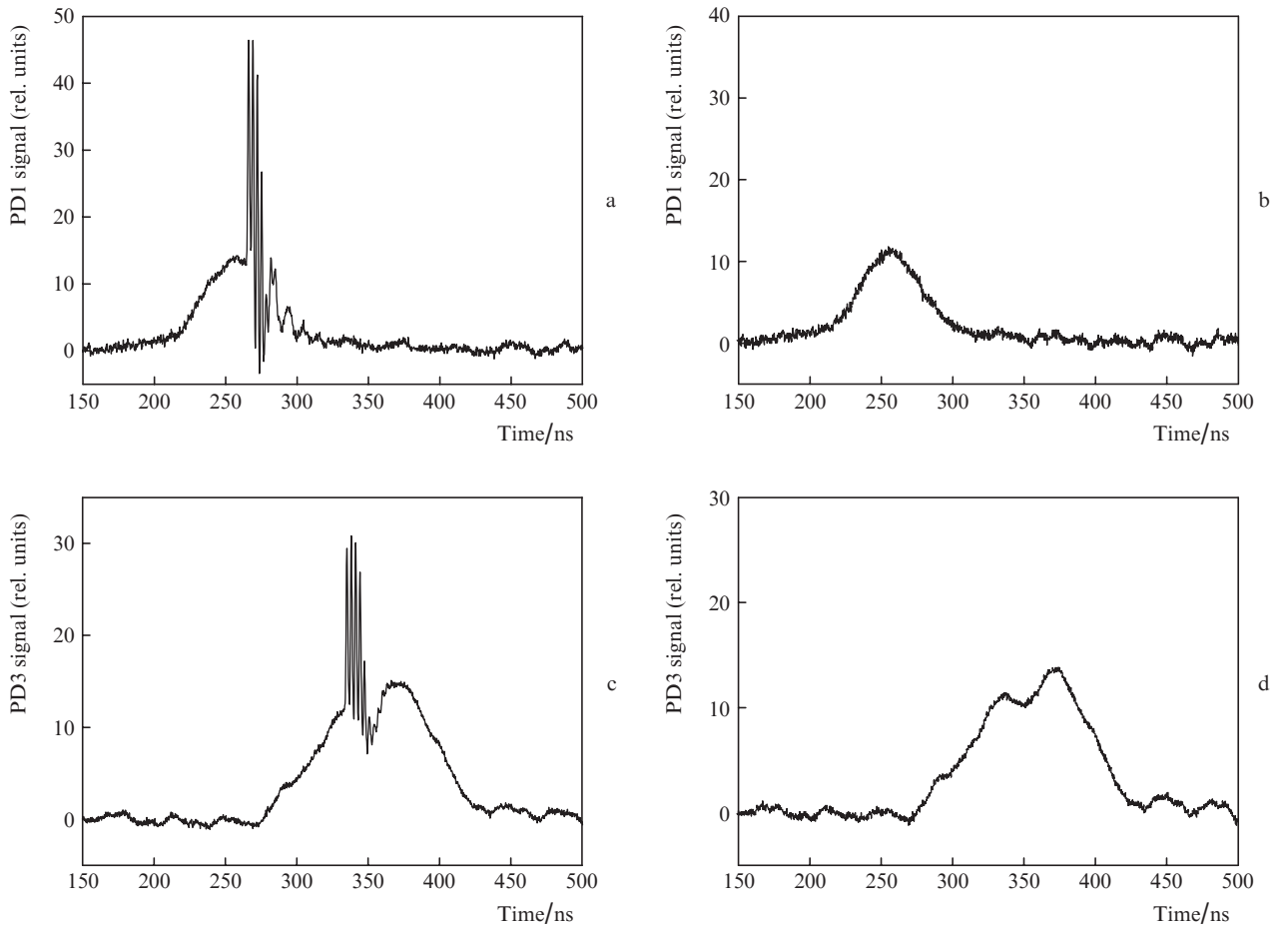

Figure 7. Oscillograms of signals from photodiodes (a, b) PD1 and (c, d) PD3 for (a, c) amplification of the USP train and (b, d) in the absence of USPs in the scheme with four passes through the Berdysh preamplifier and two passes through the GARPUN amplifier (4+2). Time is counted from the oscilloscope sweep reference point.

increase in the number of passes through the amplifiers from four (in the 2+2 scheme) to six (in the 4+2 scheme) does not lead to the desired result (significant increase in the output energy). In the ideal approximation (in the absence of ASE and other losses, except for nonsaturable intrinsic absorption in the gain medium), the output energy density for a single USP increases with an increase in the gain length to the limiting value $Q_{\rm lim} = Q_s g_0/\alpha_{\rm ns} = 20–40$ mJ cm^{-2}, which is found from the condition $d\varepsilon/dx = 0$ in Eqn (1); this condition indicates that the total energy extracted from the gain medium is entirely absorbed in this medium. For the output-aperture area $S \approx 200$ cm^2 in the GARPUN amplifier, the limiting single-USP energy should be 4–8 J and about three times larger for a train. Taking into account other losses, related to the Fresnel reflection from amplifier windows without antireflection coatings and to the radiation absorption by molecular fluorine (which is the component of the working gas mixture and absorbs laser radiation) in the unexcited state in the regions near the amplifier windows, which were not pumped by an electron beam, according to estimates, does not change the situation. Therefore, the saturation of the output energy of the USP train ($E_{\rm out} \approx 1.6$ J), which is observed with an increase in the number of passes through amplifiers, is determined by not only the saturation of the gain-medium but also the nonlinear absorption in the amplifier windows, which increases with an increase in the number of passes. Indeed, when an amplified USP train with the maximum energy passed through a 30-mm-thick CaF_2 plate (the same as the amplifier output window), the transmission was 50% (with a contribution of the Fresnel loss of the radiation reflected from two plate surfaces without antireflection coatings of about 8%). Thus, when passing through windows, the amplified USPs lose a large part of the energy extracted from the amplifier gain medium.

3. Nonlinear USP radiation loss in the KrF-amplifier windows

3.1. Estimate of nonlinear USP radiation loss in GARPUN-amplifier windows

The nonlinear losses of KrF laser radiation in different UV optical materials – fused silica (SiO_2), calcium fluoride (CaF_2), barium fluoride (BaF_2), magnesium fluoride (MgF_2), and lithium fluoride (LiF) – were previously measured in a number of studies for subpicosecond [9, 23–25] and 8-ps [26] pulses. The limitations imposed by nonlinear absorption in the windows on the limiting powers of KrF amplifiers were discussed in review [27]. Since the doubled energy of the KrF-radiation photon (10 eV) exceeds the band gaps in SiO_2 ($\Delta E = 7.8$ eV) and BaF_2 ($\Delta E = 9.1$ eV), these materials exhibit strong two-photon absorption with coefficients $\beta = (4.8–8)\times10^{-11}$ and 1.1×10^{-10} cm W^{-1}, respectively; these values are unsuitable for the windows of USP KrF amplifiers. LiF ($\Delta E = 11.6$ eV) and MgF_2 ($\Delta E = 11.8$ eV) exhibit only three-photon absorp-

tion with coefficients $\gamma = 1.6\times10^{-23}$ and 1.1×10^{-23} cm^3 W^{-2}, respectively [24]. However, high-power UV USPs [25] or X-ray bremsstrahlung (which accompanies electron beam pumping of KrF amplifiers) form long-lived colour centres in these materials; these centres are accumulated with pulses [28]. The maxima of absorption bands for colour centres in LiF and MgF_2 are near the laser wavelength 248 nm; hence, these materials are also unfit for amplifier windows. The band gap of CaF_2 coincides with the doubled energy of laser-radiation photon. In this context, there are significant discrepancies in the interpretation of the absorption mechanism (its consideration as a two-photon [23, 25] or three-photon [24, 26] process) and a large spread in the measured values of three-photon absorption coefficient: $\gamma = 2\times10^{-21}$ cm^3 W^{-2} [26] for 8-ps pulses and $\gamma = 3.8\times10^{-23}$ cm^3 W^{-2} for subpicosecond USPs [24]. It was noted in [24] that, along with the three-photon absorption, nonlinear radiation scattering (33% at an incident radiation intensity of 120 GW cm^{-2}) and the formation of colour centres also contribute to losses in CaF_2.

Let us estimate the value of three-photon absorption in CaF_2 windows based on the light propagation law

$$\frac{dI}{dx} = -\gamma I^3, \tag{2}$$

which yields an expression for the intensity of radiation transmitted through a window with a thickness l:

$$I(l) = \frac{I_0}{(1 + 2\gamma I_0^2 l)}. \tag{3}$$

If we assume the USP radiation distribution over the amplifier output window to be uniform, formula (3) for the maximum radiation intensity at the GARPUN amplifier output (averaged over the output aperture with an area $S \approx 200$ cm^2), $I_{out} = E_{out}/S\tau \cong 3.2\times10^9$ W cm^{-2}, at a window thickness $l = 3$ cm and three-photon-absorption coefficient $\gamma = 3.8\times10^{-23}$ cm^3 W^{-2} for CaF_2, yields the following estimate for the window transmission (with the Fresnel reflection disregarded): $T = I(l)/I_0 \approx 1$.

However, in the case under consideration, the peak power of amplified USPs is $P \sim 0.5$ TW [5, 21], a value exceeding by almost four orders of magnitude the critical power of beam filamentation in air: $P_{cr} = 3.8\lambda^2/(8\pi n_0 n_2) \approx 100$ MW, where $n_0 \approx 1$ and $n_2 \approx 10^{-18}$ cm^2 W^{-1} are, respectively, the linear and nonlinear refractive indices for UV light with $\lambda = 248$ nm [29, 30]. In reality, as our previous experiments showed [5, 21], a beam propagating in air consists of many filaments, which are grouped at the boundaries of blocks that form large windows of the GARPUN amplifier. The block boundaries introduce phase distortions to initiate multiple filamentation of the passing beam. In CaF_2, where $n_0 \approx 1.45$ and $n_2 \approx 1.9\times10^{-16}$ cm^2 W^{-1} for UV light ($\lambda = 308$ nm) [31], the critical filamentation power is even lower ($P_{cr} \approx 3$ MW), and a beam passing through a window should obviously undergo filamentation. Without exact knowledge of how the radiation distribution in the beam changes when outgoing from windows into the ambient air, one can nevertheless estimate the loss in the amplifier output window proceeding from the known pattern of filamentation in air.

The distribution of the radiation energy density in the cross section of a high-power beam at a distance of ~25 m from the GARPUN amplifier output was measured using a K8 glass plate, which fluoresced under UV light; the fluorescence image was recorded by a CCD video camera [32]. The dependence of the glass fluorescence intensity on the USP intensity was calibrated in independent experiments on a Ti:sapphire front-end, with variation (using a diffraction attenuator) in the USP energy from 0.14 to 0.007 mJ (a range corresponding to the change in the USP peak power from 1.4 to 0.07 GW); then the USP energy was focused by a lens with $F = 1$ m into a spot with a radiation distribution close to Gaussian.

Measurements for high-power amplified single USPs with energies $E \approx 0.2$ J (at a peak power $P \approx 0.2$ TW) showed that the number of filaments in the beam is $N_f \sim 500$; note that they contain only some fraction of radiation energy: $\varsigma = 0.3$. Thus, one filament transfers a power $P_f = 0.3P/N_f \approx 120$ MW, which approximately corresponds to the critical filamentation power P_{cr}. For filaments with a diameter (measured at a level of 1/2 of the maximum) $d_f = 290 \pm 50$ μm and average area $S_f = \pi d_f^2/4$, the peak intensity is $I_f = P_f/S_f = (1.8\pm0.6)\times10^{11}$ W cm^{-2}, which exceeds the beam intensity averaged over the amplifier output aperture ($I = P/S = 1$ GW cm^{-2}) by a factor of 200. An estimate from formula (3) yields a nonlinear decrease in the filament power in the amplifier output window corresponding to $T_f \approx 0.34$. With allowance for the scattering loss ζ, which is 0.33 for the radiation intensity in filaments comparable with that used in [24], the 'effective' reduction is even larger: $T_{eff} = (1 - \zeta)T_f = 0.23$. For the entire beam, in which filaments transfer only some part of energy (ς), the transmission $T = T_F[(1 - \varsigma) + \varsigma T_{eff}] \approx 0.7$ (here, $T_F = 0.92$ is the window transmission in the case of Fresnel reflection of light from both surfaces).

The above estimate was based on the assumption that the USP radiation distributions in the window bulk and in the ambient air are identical. However, this assumption contradicts the generally accepted idea about multiple filamentation [33], according to which individual filaments transfer power close to critical. Since P_{cr} in CaF_2 is lower than in air by a factor of 30, one might expect the number of filaments in it to be as many times larger and the total fraction of the power transferred by them to increase. Having no possibility of measuring the radiation distribution directly in the output window of the GARPUN amplifier, we investigated the transmission of an equivalent CaF_2 sample for USPs with a peak power varied in a wide range (0.01–1 GW), focused into a spot comparable in size with multiple filaments in air.

3.2. Measurement of the nonlinear loss of USP energy in CaF_2

Experiments were performed on a Ti:sapphire front-end, the radiation of which with $\lambda = 248$ nm was focused by a long-focal-length lens with $F = 2$ m into a 2-cm-thick CaF_2 sample, which was placed in the beam waist at a distance of ~8 cm from the focal plane. The USP energy at the front-end output was measured by an OPHIR calorimeter to be ~0.1 mJ for pulses ~100 fs long; this energy corresponded to $P_{max} \sim 1$ GW. The radiation incident on the sample was attenuated (step by step, using a diffraction attenuator) by a factor of 100; the spot diameter, measured by a Spiricon SP620U profilometer (OPHIR) to be ~300 μm at half maximum, was approximately the same both at the maximum USP power, which exceeded the critical filamentation power P_{cr} in air by a factor of 10, and at the minimum power, which was lower than the critical power by a factor of 10. Since the spot diameter coincided with the average diameter of individual filaments in the high-power beam of amplified USPs, the conditions allowing for the transmission of individual filaments through the amplifier window were reproduced in a much

wider range of peak powers, which obviously exceeded the critical filamentation power in CaF_2.

The radiation transmitted through the sample and a collimating diaphragm (the size of which was chosen close to the beam diameter in the absence of sample) was directed to an ASP spectrometer (Avesta Project Ltd.) with a CCD array. The integrals over the spectral distributions of the radiation transmitted through the sample and the radiation propagating in the absence of sample were compared to find the relative value of radiation transmission (reduction), caused by the total effect of nonlinear absorption and scattering. This detection technique made it possible to exclude the influence of spectral broadening of the radiation transmitted through CaF_2 on the measurement results, which was observed when using photodiodes (the spectral sensitivity on the latter depends strongly on the radiation wavelength in the UV region). Note that strongly attenuated radiation also could not be measured directly by a calorimeter because of the insufficient sensitivity of the latter.

Figure 8 presents characteristic radiation spectra (normalised to the maximum intensities) in the absence of a CaF_2 sample and after transmission through a sample, for incident USPs with energy of 0.045 mJ (peak power 0.45 GW). It can be seen that the spectrum in CaF_2 is broadened by a factor of about 2 in comparison with the spectrum in air. A rather large fraction of energy (to several tens of percent) is concentrated in wide wings, the half-width of which, $\Delta\lambda_{1/2} \sim 20$ nm, greatly exceeds the gain band of the KrF laser transition (~2.5 nm). In air, the integral over the spectrum of radiation transmitted through the focal waist (where one would also expect some part of radiation to be absorbed) depended linearly on the incident energy. The USP energy measured directly by a calorimeter, with zero reduction of diffraction attenuator, was the same before and after the beam waist, due to which the values of the integrals could be calibrated with respect to the spectrum by relating them to the incident energy or USP power. The results of this processing, with allowance for the Fresnel reflection from both sample surfaces, are shown in Fig. 9. It can be seen that significant nonlinear losses arise in CaF_2 for USPs with a peak power exceeding 0.1 GW, a value corresponding to an incident radiation intensity of $\sim 1.5\times10^{11}$ W cm^{-2}. With an increase in the USP power, the nonlinear losses increase and reach 80% of the incident power at $P = 1$ GW.

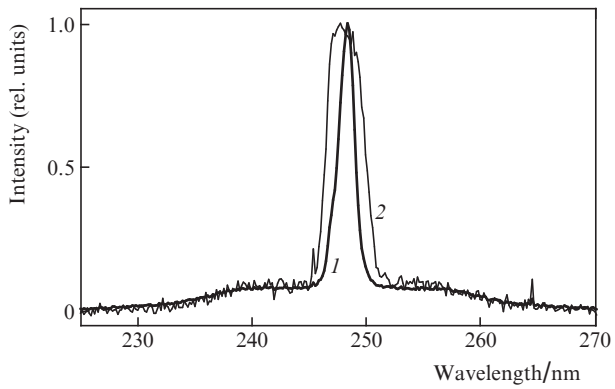

Figure 8. Spectra of USP radiation (*1*) in the absence of sample and (*2*) after transmission through a CaF_2 sample at a peak USP power of 0.45 GW.

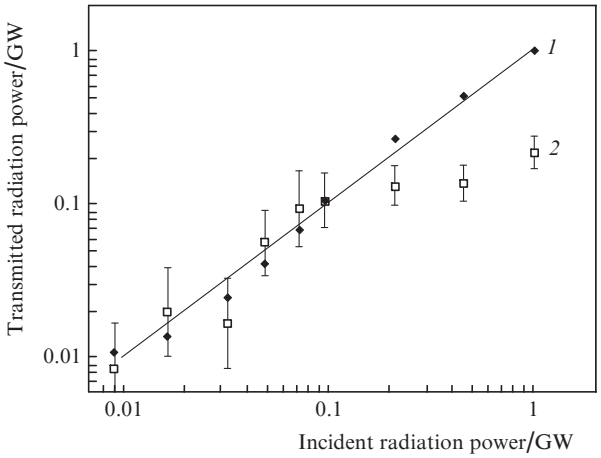

Figure 9. Dependences of the (*1*) air and (*2*) CaF_2 transmission on the USP power.

The results of the above-described experiments qualitatively confirm our measurements (Subsection 2.3) and estimates of nonlinear losses for a high-power, strongly filamented USP beam in the windows of GARPUN KrF amplifier (Subsection 3.1), obtained based on the data of [24]. The UV radiation intensities at which nonlinear absorption and scattering in CaF_2 manifest themselves are close to those reported in [23,27]. Note that another possible cause of the loss in the amplifier windows is the experimentally observed strong broadening of the spectrum, as a result of which its width exceeds that of the gain band of the KrF laser transition.

3.3. Measurement of the induced absorption in CaF_2

The induced absorption in the windows of the GARPUN amplifier, which is related to the generation of colour centres in CaF_2, contributed little to the nonlinear three-photon absorption and scattering; however, it accumulated from pulse to pulse. Probing the output window with an electric-discharge KrF laser showed that the initial transmission ~90% (close to the Fresnel transmission) reduced to 72% after several hundreds of USPs and the transmission of the opposite window, which operated at lower USP powers, decreased to 84%. A long-term (~6 h) annealing of windows in a muffle furnace at a temperature of 350 °C and their subsequent polishing (to remove the surface defect layer formed as a result of interaction of heated CaF_2 with atmospheric air) made it possible to recover the initial window transmission.

4. Conclusions

Different multipass schemes of amplification of subpicosecond USPs in two cascades of wide-aperture KrF amplifiers with electron beam pumping were investigated on the GARPUN-MTW Ti:sapphire/KrF hybrid laser facility. For specific pump powers $W_b = 0.6-0.8$ MW cm^{-3}, the small-signal gain in the amplifiers was found to be $g_0 = 0.08-0.10$ cm^{-1} [1,5,21]. It was shown that for a USP repetition period of 3–5 ns, which exceeds the gain-medium recovery time (~2 ns), the train is amplified in the same way as for a single USP. Due to this, a train can efficiently extract the pump energy from amplifiers and sum the energies of individual USPs. When a 4-pulse USP train with a total energy $E_{in} \sim 0.1$ mJ was amplified in four passes through the Berdysh preamplifier and in two passes

through the final GARPUN amplifier (4+2 scheme), the output USP energy was saturated at E_{out} = 1.6 J and corresponded to the maximum USP peak powers ~0.6 TW. The ASE energy, on the contrary, rapidly increased at the large total gain length $L_{eff} \approx 600$ cm (at $g_0 L_{eff} \sim 60$) and amounted to 50% of the total output energy. In the (4+1) and (2+2) schemes, the USP energy decreased only slightly (to E_{out} = 1.3 and 1.2 J), and the ASE fraction decreased to 10% and 3%, respectively.

The saturation of the USP output energy with an increase in the number of passes through amplifiers was determined to a great extent (along with the gain saturation and loss in the gain medium) by the nonlinear loss in the CaF_2 windows, caused by the nonlinear absorption, scattering, and broadening of the radiation spectrum to a value exceeding the gain band of the KrF laser transition. The nonlinear loss in the output windows enhanced the self-focusing of USPs, the peak power of which was almost four orders of magnitude higher than the critical power of filamentation in air and five orders of magnitude higher than the critical power of filamentation in CaF_2. The experimentally observed multiple filamentation of the laser beam initiated by phase distortions at the boundaries of blocks that formed the large windows of the final amplifier. The filamentation led to a 200-multiple local increase in the radiation intensity in filaments (approximately to 2×10^{11} W cm^{-2}). Suppression of filamentation and decrease in the nonlinear loss in the KrF amplifier windows should increase the USP output energy. To this end, it is expedient to reduce the number of USP passes through windows in multipass schemes and use internal mirrors, mounted directly on amplifiers. These windows must be thinner and made of CaF_2 single crystals. To transport a high-power beam between cascades, one should apply tubes evacuated to forevacuum or filled with helium, which has a low nonlinear refractive index. The problem of beam filamentation can be radically solved by amplifying chirped pulses in KrF amplifiers with their subsequent compression; this approach was demonstrated in [34, 35].

Acknowledgements. We are grateful to E.A. Sunchugasheva for her help in the preparation of experiments.

This work was supported by the Programmes of Fundamental Research 'Fundamental Problems of Pulsed High-Current Electronics' and 'Extreme Light Fields and Their Applications' of the Presidium of the Russian Academy of Sciences.

References

1. Zvorykin V.D., Didenko N.V., Ionin A.A., et al. *Laser Part. Beams*, **25**, 435 (2007).
2. Foldes I.B., Szatmari S. *Laser Part. Beams*, **26**, 575 (2008).
3. Bouma B., Luk T.S., Boyer K., Rhodes C.K. *J. Opt. Soc. Am. B*, **10**, 1180 (1993).
4. Nabekawa Y., Sajiki K., Yoshitomi D., et al. *Opt. Lett.*, **21**, 647 (1996).
5. Zvorykin V.D., Levchenko A.O., Ustinovskii N.N. *Kvantovaya Elektron.*, **41**, 227 (2011) [*Quantum Electron.*, **41**, 227 (2011)].
6. Kryukov P.G. *Kvantovaya Elektron.*, **31**, 95 (2001) [*Quantum Electron.*, **31**, 95 (2001)].
7. Korzhimanov A.V., Gonoskov A.A., Khazanov E.A., Sergeev A.M. *Usp. Fiz. Nauk*, **181**, 9 (2011).
8. Molchanov A.G. Trudy FIAN, 171, 54 (1986).
9. Endoh A., Watanabe M., Sarucura N., Watanabe M. *Opt. Lett.*, **14**, 353 (1989).
10. Divall E.J., Edwards C.B., Hirst G.J., et al. *J. Mod. Opt.*, **43**, 1025 (1996).
11. Shaw M.J., Ross I.N., Hooker C.J., et al. *Fusion Eng. Des.*, **44**, 209 (1999).
12. Zvorykin V.D., Lebo I.G., Rozanov V.B. *Kratk. Soobshch. Fiz., FIAN*, (9–10), 20 (1997).
13. Zvorykin V.D., Ionin A.A., Levchenko, et al. *Kvantovaya Elektron.*, **43**, 332 (2013) [*Quantum Electron.*, **43**, 332 (2013)].
14. Ionin A.A., Kudryashov S.I., Levchenko A.O., et al. *Appl. Phys. Lett.*, **100**, 104105 (2012).
15. Zvorykin V.D., Ionin A.A., Levchenko A.O. *Kvantovaya Elektron.*, **43**, 339 (2013) [*Quantum Electron.*, **43**, 339 (2013)].
16. Zvorykin V.D., Levchenko A.O., Ustinovskii N.N. *Kvantovaya Elektron.*, **41**, 227 (2011) [*Quantum Electron.*, **41**, 227 (2011)].
17. Zvorykin V.D., Levchenko A.O., Shutov A.V., et al. *Phys. Plasmas*, **19**, 033509 (2012).
18. Sethian J.D., Friedman M., Jiuliani Jr. J.L., et al. *Phys. Plasmas*, **10**, 2142 (2003).
19. Lehmberg R.H., Giuliani J.L., Schmitt A.J. *J. Appl. Phys.*, **106**, 023103 (2009).
20. Obenschain S.P., Sethian J.D., Schmitt A.J. *Fusion Sci. Tech.*, **56**, 594 (2009).
21. Zvorykin V.D., Ionin A.A., Levchenko A.O., et al. *J. Phys. Conf. Ser.*, **244**, 032014 (2010).
22. Tilleman M.M., Jacob J.H. *Appl. Phys. Lett.*, **50**, 121 (1987).
23. Taylor A.J., Gibson R.B., Roberts J.R. *Opt. Lett.*, **13**, 814 (1988).
24. Simon P., Gerhardt H., Szatmari S. *Opt. Lett.*, **14**, 1207 (1989).
25. Hata K., Watanabe M., Watanabe S. *Appl. Phys. B*, **50**, 55 (1990).
26. Tomie T., Okuda I., Yano M. *Appl. Phys. Lett.*, **55**, 325 (1989).
27. McIntire I.A., Rhodes C.K. *J. Appl. Phys.*, **69**, R1 (1991).
28. Zvorykin V.D., Alimov A.S., Arlantsev S.V., et al. *Plasma Fus. Res.*, **8**, 2405000 (2013).
29. Schwarz J., Rambo P., Diels J.C., et al. *Opt. Commun.*, **180**, 383 (2000).
30. Tzortzakis S., Lamouroux B., Chiron A., et al. *Opt. Commun.*, **197**, 131 (2001).
31. Kim Y.P., Hutchinson M.H.R. *Appl. Phys. B*, **49**, 469 (1989).
32. Zvorykin V.D., Ionin A.A., Levchenko A.O., et al. *Nucl. Instrum. Methods Phys. Res. B*, **309**, 218 (2013).
33. Couairon A., Mysyrowicz A. *Phys. Rep.*, **441**, 47 (2007).
34. Houliston J.R., Ross I.N., Key M.H., et al. *Opt. Commun.*, **104**, 350 (1994).
35. Ross I.N., Damerell A.R., Divall E.J. *Opt. Commun.*, **109**, 288 (1994).